

## Design and control of novel reaction–separation–recycle processes for the production of 4-hydroxybutyl acrylate

Moraru, Mihai Daniel; Kiss, Anton A.; Bildea, Costin Sorin

**DOI**

[10.1016/j.cherd.2021.11.040](https://doi.org/10.1016/j.cherd.2021.11.040)

**Publication date**

2022

**Document Version**

Final published version

**Published in**

Chemical Engineering Research and Design

**Citation (APA)**

Moraru, M. D., Kiss, A. A., & Bildea, C. S. (2022). Design and control of novel reaction–separation–recycle processes for the production of 4-hydroxybutyl acrylate. *Chemical Engineering Research and Design*, 177, 801-814. <https://doi.org/10.1016/j.cherd.2021.11.040>

**Important note**

To cite this publication, please use the final published version (if applicable). Please check the document version above.

**Copyright**

Other than for strictly personal use, it is not permitted to download, forward or distribute the text or part of it, without the consent of the author(s) and/or copyright holder(s), unless the work is under an open content license such as Creative Commons.

**Takedown policy**

Please contact us and provide details if you believe this document breaches copyrights. We will remove access to the work immediately and investigate your claim.

***Green Open Access added to TU Delft Institutional Repository***

***'You share, we take care!' - Taverne project***

**<https://www.openaccess.nl/en/you-share-we-take-care>**

Otherwise as indicated in the copyright section: the publisher is the copyright holder of this work and the author uses the Dutch legislation to make this work public.



ELSEVIER

Contents lists available at ScienceDirect

Chemical Engineering Research and Design

journal homepage: [www.elsevier.com/locate/cherd](http://www.elsevier.com/locate/cherd)

# Design and control of novel reaction–separation–recycle processes for the production of 4-hydroxybutyl acrylate



Mihai Daniel Moraru<sup>a,\*</sup>, Anton A. Kiss<sup>b,c</sup>, Costin Sorin Bildea<sup>d</sup>

<sup>a</sup> Hexion, Department of Technology, Engineering and Projects, Seattleweg 17, 3195 ND Pernis, The Netherlands

<sup>b</sup> Department of Chemical Engineering, Delft University of Technology, Van der Maasweg 9, 2629 HZ Delft, The Netherlands

<sup>c</sup> Department of Chemical Engineering and Analytical Science, The University of Manchester, Sackville Street, Manchester M13 9PL, United Kingdom

<sup>d</sup> University Politehnica of Bucharest, Department of Chemical and Biochemical Engineering, Str. Gh. Polizu 1-7, 011061 Bucharest, Romania

## ARTICLE INFO

### Article history:

Received 2 September 2021

Received in revised form 22 November 2021

Accepted 30 November 2021

Available online 8 December 2021

### Keywords:

Acrylic acid

Esterification

Hydrolysis

Pressure-swing distillation

## ABSTRACT

Two chemistry routes are known for 4-hydroxybutyl acrylate production: the direct esterification of acrylic acid with 1,4-butanediol, and the transesterification of methyl acrylate with 1,4-butanediol. However, very scarce information in the literature is available about industrial production, or design and operation of production processes. In this study, we propose three novel reaction–separation–recycle processes for 4-hydroxybutyl acrylate production by direct esterification based on solid catalyst. Use of solid catalysts may avoid well-known issues of the liquid catalysts like recovery and re-use of the catalyst, difficult product recovery, and corrosion. Due to the nature of the chemical system and reactions conditions, the chemistry is not 100% selective towards the acrylate, important amounts of diacrylate by-product being formed. All processes use fixed-bed tubular reactors to perform the reactions and distillation-based equipment to achieve the required separations. While all processes have a similar separation sequence, each has its key particularities: the RSR-A process accepts the loss of reactants due to formation and elimination from the process of the diacrylate, RSR-B converts the diacrylate into its reactants in the esterification reactor, while RSR-C converts the diacrylate in a dedicated hydrolysis reactor. A key element in the separation sequence is the use of pressure-swing distillation to make the difficult split of the alcohol/acrylate/diacrylate ternary mixture. All processes are capital and energy intensive. The economic analysis shows that the RSR-A process has the most favorable economics: a total annualized cost of 2 million \$/y and a specific annualized cost of 100 \$/t of product. A control structure for the RSR-C process is presented, the dynamic simulations showing its efficiency in rejecting various disturbances.

© 2021 Institution of Chemical Engineers. Published by Elsevier B.V. All rights reserved.

## 1. Introduction

Acrylates are essential chemicals of much interest as they are bifunctional: the carboxylate group has numerous functionalities while the

vinyl group is prone to polymerization. Hydroxyalkyl acrylates are useful for fiber treating agents, dyeability improving agents, coatings, anti-static additives, adhesives, raw materials for resins, and precursors for various organic compounds. Among them, 4-hydroxybutyl acrylate (HBA) is used to obtain homopolymers and copolymers with end-use in a variety of products (e.g. coating, photosensitive resins, pressure sensitive additives). HBA is also used in chemical syntheses, because it readily undergoes addition reactions with a wide variety of

\* Corresponding author.

E-mail address: [mihai.moraru@hexion.com](mailto:mihai.moraru@hexion.com) (M.D. Moraru).

<https://doi.org/10.1016/j.cherd.2021.11.040>

0263-8762/© 2021 Institution of Chemical Engineers. Published by Elsevier B.V. All rights reserved.

organic and inorganic compounds (BASE, 2016a,b). Typical industrial specifications are min. 97% purity, max. 0.3% acrylic acid, max. 0.5% diacrylate and max. 0.1% water content, all by mass.

Two chemistry routes to produce HBA are the direct esterification of acrylic acid (AA) with 1,4-butanediol (BD), and transesterification of methyl acrylate (MA) with BD. Water is a by-product of the direct esterification, while methanol is a by-product of the transesterification route. Another by-product, which is formed in both chemistry routes, is 1,4-butanediol diacrylate (BDA), formed between the AA reactant and HBA product; water is also obtained in this esterification reaction. More information on secondary reactions is presented in the paper of Ostrowski et al. (2011). The authors use the density-functional theory (a computational quantum mechanical modelling method) to calculate, among others, the activation energy of four secondary reactions of several esterification systems. In the order of increasing the activation energy, these side reactions are (i) the addition of AA to the double bond in acrylates, (ii) additions of water and alcohols to acrylates, (iii) dimerization of AA, and (iv) addition of alcohol to the acid dimer, which leads to the same product as the addition of AA to an acrylate. Relative to one another, the lower the activation energy, the easier that reaction occurs; therefore, the by-product formation of the lower activation energy-reactions are favored.

Most of the information about these routes and how to prepare HBA are found in the patent literature. A patent by BASF (Dockner et al., 1995) describes the preparation of 1,4-butanediol mono-acrylate by esterification of acrylic acid with 1,4-butanediol, by a process leading to an aqueous solution of unconverted BD, which is converted into tetrahydrofuran (THF) in the presence of a catalytic amount of a strong acid and THF is separated off from the aqueous solution. Rohm and Haas Co. (Curtis, 2008) claimed an improved chemical process which can yield high purity hydroxyalkyl acrylates from acrylic acid and alkylene oxides. Similar methods for producing a hydroxyalkyl acrylates by reacting acrylic acid with an alkylene oxide were disclosed by Mitsubishi Chemical (Tokuda et al., 2009) and Nippon Shokubai (Jinno et al., 2015).

Osaka Organic Chemical Industry Co. Ltd. (Sugiura et al., 2013) claimed a process for preparing 4-hydroxybutyl acrylate by transesterification of an alkyl acrylate with 1,4-butanediol in the presence of a dialkyltin oxide. A more recent patent (Tanaka et al., 2017) from the same company describes that HBA can be produced by transesterification of MA with BD in the presence of a dialkyltin oxide (e.g., dioctyltin oxide, dilauryltin oxide, dibutyltin oxide) serving as catalyst. This reaction is made in the presence of a solvent (e.g., cyclohexane, methylcyclohexane) and inhibitor (e.g. phenothiazine) to minimize polymerization. The patent claims that the catalyst can be recovered and reused. The same patent (Tanaka et al., 2017) gives some details also on the direct esterification reaction, mentioning that by-products formation is great, the process has a complicated neutralizing step because a homogeneous acid (sulfonic acid or para-toluene sulfonic acid) is used as a catalyst, and that salts generated in large amounts in the neutralizing step become wastes. In addition, the unreacted AA remains in the HBA product preventing its use as raw material in some high-end applications.

A relatively recent journal article (Yang et al., 2008a) shows that the direct esterification reaction can also be performed using a solid catalyst, namely Amberlyst 15, which is a strongly acidic ion-exchange resin. In this way, the well-known issues of the liquid catalysts (e.g. recovery and re-use of the catalyst, difficult product recovery, corrosion, and other environmental problems during the disposal of waste) may be avoided. Yet, it remains challenging due to the secondary reaction leading to the unwanted BDA by-product.

Although this reaction was performed in the laboratory using a solid-based catalyst, the possibility to apply this reaction at industrial scale has not been investigated. To the best of our knowledge, the open literature neither presents conceptual process design studies nor describes existing industrial processes for HBA production; note that a preliminary conceptual design was reported in our recent conference paper (Moraru et al., 2020). Important issues such as reactor type and size (mass of catalyst) and operating conditions (temperature, reactant ratios), structure of the separation section (separation sequence and

number of columns), sizing of the separation units, utilities requirement and economic evaluations are missing. The goal of this paper is to fill this research gap.

In this context, the design of three novel reaction–separation–recycle (RSR) processes are developed and presented in this study. The estimation of reaction kinetic parameters using experimental data reported in the literature (Yang et al., 2008a) is made first. Then, the thermodynamic model and the key physical properties are presented. Based on a kinetic reactor model, a black-box (ideal) separation section and recycle of unconverted reactants, a preliminary analysis of the RSR system is made. Major choices regarding BDA recovery, recycle and reaction lead to the creation of three distinct RSR systems. The selection of an initial operating point (for each of the systems) provides the mass balance for the synthesis of the separation system. The study ends with an economic-based comparison of the three processes, dynamics and control of one of the processes, and general conclusions. The proposed plant has a capacity of 20 kt/a of HBA. The product specifications are 99.5% HBA. Aspen Plus V10 (AP) and its utilities are used as efficient computer-aided process engineering (CAPE) tools to perform the process design and economic analysis.

## 2. Reactions and kinetics

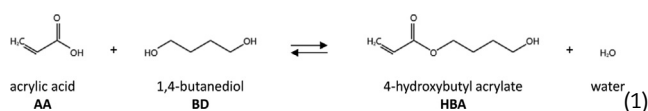
The aim of this chapter is to derive a kinetic model describing the main reactions of the HBA production process. Yang et al. (2008a) performed experimental work to study the course of two most important reactions describing this process. The authors also proposed a concentration-based (power law) kinetic model and determined the values of the kinetic parameters: the two pre-exponential constants of the Arrhenius equation, the activation energies of the two reactions, and the experimental concentration-based equilibrium constants.

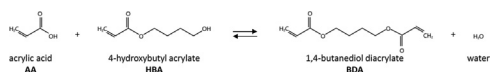
However, we observe a large discrepancy between the experimental data and the calculated data using the aforementioned model. Our conclusion is that this difference comes from the values of the two pre-exponential constants; our first estimations (not detailed here) indicate that these constants should be higher by a factor of 1000. The activation energies of the two reactions seem reasonable and similar to those of other esterification reactions of the same kind presented in the literature; we retain in our calculations the values of the activation energies reported by the authors.

Due to this discrepancy, we use the experimental data provided in the same paper (Yang et al., 2008a) and regress the pre-exponential constants for the same kinetic model. Details are presented in Sections 2.1 and 2.2.

### 2.1. Literature experimental data and kinetic model equations

The chemistry of the HBA production is complex, involving many reactions with formation of various undesired by-products. Generally, it is known that use of inhibitors reduces the formation of by-products. The paper of Yang et al. (2008a) describes the HBA production using two esterification reactions: the main reaction with formation of desired HBA (Eq. (1)) and a secondary reaction with formation of undesired BDA (Eq. (2)); undesired water is formed in both reactions. Both are equilibrium-limited reactions. The kinetic model proposed in that paper is described by Eqs. (3)–(8).





(2)

$$r_1 = k_1 (C_{AA} C_{BD} - (1/K_{eq,1}) C_{HBA} C_{water}) \quad (3)$$

$$\ln(K_{eq,1}) = B_1/T + A_1 \quad (4)$$

$$k_1 = k_{0,1} \exp(-E_{A,1}/RT) \quad (5)$$

$$r_2 = k_2 (C_{AA} C_{HBA} - (1/K_{eq,2}) C_{BDA} C_{water}) \quad (6)$$

$$\ln(K_{eq,2}) = B_2/T + A_2 \quad (7)$$

$$k_2 = k_{0,2} \exp(-E_{A,2}/RT) \quad (8)$$

In Eqs. (3)–(5) the variables subscript 1 refers to the first reaction, while in Eqs. (6)–(8) the subscript 2 refers to the second reaction.  $r$  [kmol/(kg<sub>cat</sub>·s)] is the reaction rate,  $k$  [kmol/(kg<sub>cat</sub>·s)/(kmol/m<sup>3</sup>)<sup>2</sup>] is the forward rate constant,  $C_i$  ( $i$ =water, AA, BD, HBA, BDA) are the liquid phase molar concentrations [kmol/m<sup>3</sup>], while  $K_{eq}$  [–] is the molar concentration-based equilibrium constant.  $k_0$  [kmol/(kg<sub>cat</sub>·s)/(kmol/m<sup>3</sup>)<sup>2</sup>] is the pre-exponential factor in the Arrhenius equation, and  $E_A$  [kJ/kmol] is the activation energy.  $R$  (=8.314 kJ/kmol/K) is the gas constant.  $A$  [–] and  $B$  [K] are constants in the equilibrium constant equations. Note that while the kinetic model is the same, Yang et al. (2008a) use different units for the various constants.

Yang et al. (2008a) studied the course of this reaction process in the presence of a solid catalyst (i.e., Amberlyst 15, a strongly acidic ion-exchange resin). The experiments were performed in a batch reactor. In a typical experiment, known amounts of reactants, mass of catalyst and inhibitor were used, and the reaction was performed at different temperatures. A summary of all the experimental conditions were provided in Table 1 of their paper.

The experimental results were reported as the evolution of HBA yield and HBA selectivity during the course of reaction. Note that the yield and selectivity together with the initial charge of the experiment represent sufficient information to fully describe an experiment. However, not all results were reported in their paper. Thus, only a limited set of experimental data are available for regressing the two pre-exponential constants of the kinetic model. Specifically, the results useful in regressing these parameters are for those experiments performed at 100 and 110 °C, for a catalyst concentration of 1.63% mass and molar ratio AA/BD of 1.85/1. For the same catalyst concentration and initial molar ratio, partial results (i.e., only yield; selectivity not reported) are also available for experiments performed at 120 °C; data at 120 °C are not used in the regression. The data used in regression are retrieved from the paper of Yang et al. (2008a) as follows:

- Data at 100 °C: yield from Fig. 9 and selectivity from Fig. 12
- Data at 110 °C: yield from Fig. 9 and selectivity from Fig. 14

Note that prior to executing the actual regression (see details in Section 2.2.2), the yield and selectivity data are manipulated to obtain the time–concentration profiles of all components (i.e., mole fractions). This is necessary since the yield and selectivity data cannot be used as such. Data used to determine the constants in the equilibrium constant equations are taken from Fig. 7 of the aforementioned paper.

## 2.2. Kinetic parameters

### 2.2.1. Regression of equilibrium constants

The four constants  $A_1$ ,  $B_1$ ,  $A_2$  and  $B_2$  in the equilibrium constant Eqs. (4) and (7) are determined using data provided in Fig. 7. After reading the data from the figure, a linear regression is made to obtain the value of these constants. The constants can be easily identified from the regression equations presented here in the Supplementary material. These values are also presented in Table 1, in which all the parameters of the kinetic model are gathered.

### 2.2.2. Regression of pre-exponential constants

The regression of the pre-exponential constants  $k_{0,1}$  and  $k_{0,2}$  in Eqs. (5) and (8) is made in Aspen Plus using the BatchOp reactor model and the Data Fit tool. Details on the regression algorithm can be found in Aspen Plus product documentation. The set-up of the regression case is as follows. Firstly, the reactions stoichiometry is included, and the reactions are specified as kinetic using the power law type kinetic expression. This consists of implementing:

- The pre-exponential constants  $k_{0,1}$  and  $k_{0,2}$ , for which some initial guesses are specified.
- The activation energies  $E_{A,1}$  and  $E_{A,2}$ , their values being as determined by Yang et al. (2008a); see here Table 1 in which all the parameters of the kinetic model are gathered.
- The driving force, which includes the parameters of the equilibrium constants  $A_1$ ,  $B_1$ ,  $A_2$  and  $B_2$ , their values being those determined in Section 2.2.1.

The setup continues with introducing the experimental data. As mentioned, the HBA yield and HBA selectivity data are transformed into time–mole fractions profiles, and the latter introduced in the regression setup. A typical entry requires the reactor initial conditions (initial charge: temperature, pressure, reactants AA + BD amounts, and catalyst amount) and the variation of components mole fraction during the course of reaction.

### 2.2.3. Kinetics results

Table 1 gathers all parameters used in the kinetic model, while Fig. 1 shows the comparison between the experimental and calculated components molar fractions. For a direct comparison of the yield and selectivity data provided in the paper of determined by Yang et al. (2008a), we provide these data in the Supplementary material. As previously mentioned, only data at 100 °C and 110 °C are used to regress the pre-exponential constants. At these particular temperatures, a good agreement between the experimental and calculated data is observed. The partial experimental data (i.e., molar fractions of HBA) at 120 °C are not used in any regression. These data compare fairly well with the calculated data in the first 200 min from the start of the experiment and begin to deviate towards the end of the experiment; this may indicate that other secondary reactions may start to become important at higher temperatures and long residence times. Note that these calculations are made for a temperature outside the temperature range in which the pre-exponential factors are regressed.

**Table 1 – Parameters of the kinetic model based on the paper of Yang et al. (2008a).**

Reaction	$E_A$ [kJ/kmol]	A [–]	B [K]	$k_0$ [kmol/(kg <sub>cat</sub> ·s)/(kmol/m <sup>3</sup> ) <sup>2</sup> ]
1	58,300	–2.0212	1457.6	91.5
2	86,700	–0.4614	810.36	181,625

Notes:  $E_A$  — as reported by Yang et al. (2008a).

A and B — determined by regression using experimental data (see Section 2.2.1).

$k_0$  — determined by regression using experimental data (see Section 2.2.2).

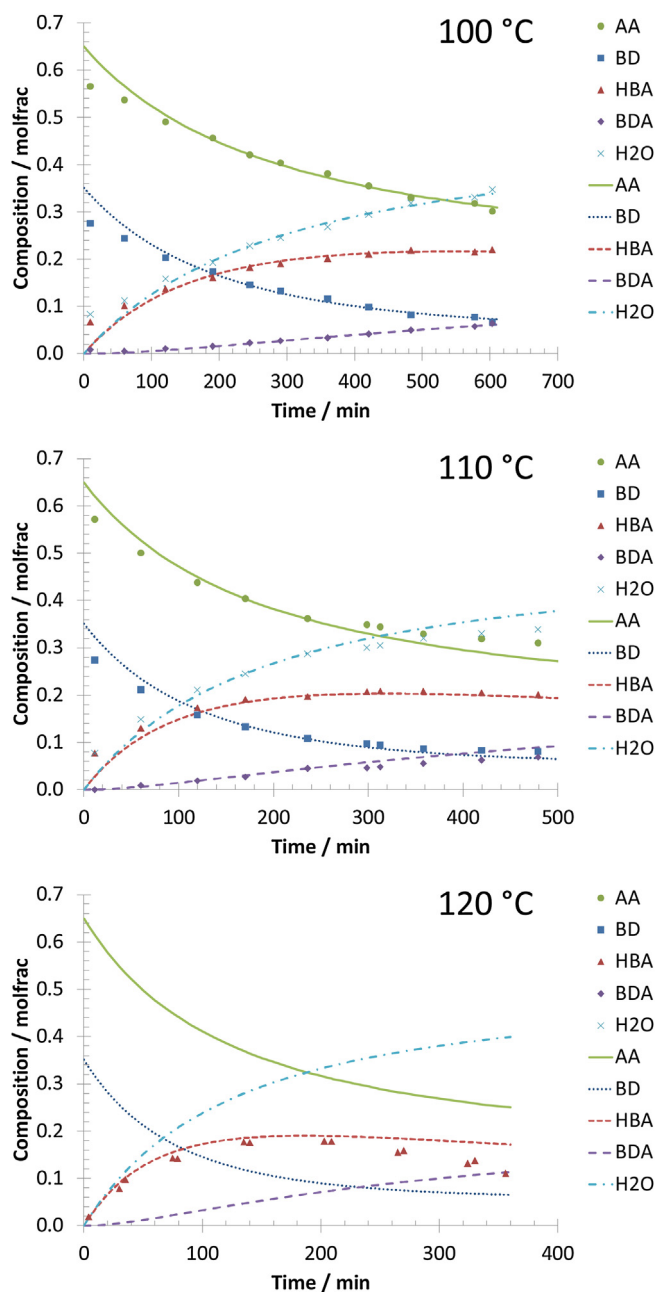


**Fig. 1 – Comparison between experimental (markers) and calculated (lines) data of component mole fraction in time at different temperatures; the initial AA:BD mole ratio (1.85:1), catalyst concentration (1.63% mass) are the same for all experiments. The experimental data are taken from the paper of Yang et al. (2008a).**

### 3. Thermodynamics

#### 3.1. Thermodynamic method

The UNIQU-HOC method in Aspen Plus (default naming) is used to calculate all properties required for the process simulation. This method uses the UNIQUAC activity coefficient model for describing the liquid phase behavior, while the vapor phase is described by the HOC (Hayden-O’Connell) equation of state model. Both the vapor–liquid equilibrium (VLE) and liquid–liquid equilibrium (LLE) use the same sets of binary interaction parameters of the activity coefficient model.

The system contains five chemical components (water, AA, BD, HBA and BDA). Out of these, only three (water, AA and BD) are present in the Aspen Plus database; all pure-component physical properties for these components are in the database. The properties for the other two components (HBA and BDA) are estimated by the Property Constant Estimation System (PCES) of Aspen Plus, based on their molecular structure. One exception is the vapor pressure of HBA (see Section 3.2). Out of the 10 binary interaction parameter sets for the UNIQUAC activity coefficient model, only two are available in the Aspen Plus database; namely, the water/AA and water/BD pairs. All the other parameters are estimated using the UNIFAC group contribution method. As Aspen Plus is a proprietary product, only the databanks name from where the parameters are retrieved is indicated (i.e. APV100 and NISTV100). The association parameter for water/AA used in the equation of state is also available in Aspen Plus databanks.

#### 3.2. Vapor pressure

The vapor pressure of water, AA and BD are well described in the Aspen database. There are no experimental data for BDA; hence, methods based on the molecular structure are used to estimate its vapor pressure. For HBA, the Antoine constants for the vapor pressure equation are determined from data presented in two BASF brochures (BASF, 2016a,b). A vapor pressure graph for all components is presented in the Supplementary material. Water and AA are the lightest, while BDA is the heaviest component in the system, suggesting easy vapor–liquid-based separations from mixtures. Two observations are that BD and HBA have very similar boiling points, and that BD is lighter at higher pressures and vice-versa at lower pressures. This behavior indicates a difficult split between the two components. This is important since BD is a reactant that needs to be recycled to the reaction section, while HBA is the product that needs to be obtained at high purity.

#### 3.3. Azeotropy and phase equilibria

The azeotropes are also important in developing the separation systems. Several azeotrope searches, using the Distillation Synthesis tool in Aspen, reveal that this five-component sys-

**Table 2 – Calculated singular points (SP): azeotropes and boiling points (mass based) at 1.013 and 0.05 bar.**

SP #	Type	Temp/[C]	H2O	AA	BD	HBA	BDA
1.013 bar							
1	het	100.0	0.978				0.022
2	hom	100.0	1				
3	hom	141.2		1			
4	hom	223.7			0.627		0.373
5	hom	225.9			0.611	0.389	
6	hom	227.8			1		
7	hom	236.0				1	
8	hom	264.8					1
0.05 bar							
1	hom	32.9	1				
2	hom	63.9		1			
3	het	142.0			0.490		0.510
4	hom	143.9			0.355	0.645	
5	hom	146.6				1	
6	hom	148.3			1		
7	hom	163.5					1

tem has azeotropes at both lower and higher pressures. We report in Table 2 the azeotropes and boiling points data at 1.013 and 0.05 bar. The close-boiling components BD and HBA form a minimum-boiling homogeneous azeotrope (azeotrope #5 at 1.013 bar, and #4 at 1.013 bar) that presents a significant change in composition from one pressure to another. The same holds also for the BD and BDA azeotrope. This can be exploited in a pressure-swing distillation system to split this ternary mixture. Ternary vapor–liquid diagrams are presented in Section 5, showing how these are used to achieve the aforementioned split. Another aspect worth mentioning is that the water–BD–BDA ternary presents liquid–liquid immiscibility; this is shown in the Supplementary material. Neither AA, nor HBA present immiscibility with the other components.

#### 4. Reaction–separation–recycle system

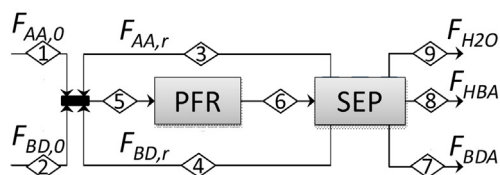
The first objective of this chapter is to establish the basic reaction–separation–recycle (RSR) structure of the process; three structures are proposed. The other objective is to select the reactor size that meets the production capacity, as well as providing an initial mass balance for the purpose of starting the design of the separation system.

##### 4.1. Basic process structure

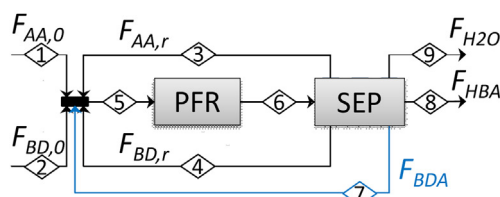
Fig. 2 presents three reaction–separation–recycle (RSR) basic process structures for the HBA production plant:

- In the RSR-A structure, the fresh ( $F_{AA,0}$ ,  $F_{BD,0}$ ) and recycled reactants ( $F_{AA,r}$ ,  $F_{BD,r}$ ) are mixed and fed to a fixed-bed tubular reactor (PFR). From the separation section (SEP), water ( $F_{H2O}$ ), HBA ( $F_{HBA}$ ) and BDA ( $F_{BDA}$ ) are removed from the system, while AA and BD are recovered and recycled to the reactor as two separate streams. This choice, with two recycle streams, has as basis the boiling temperature of pure components and azeotropes (see Table 2). Water is the lightest and can be separated first. The azeotrope with BDA does not influence this separation. Only small BDA amounts will be carried out with the water stream due to its very low concentration in the azeotrope. Similarly, AA can be easily separated from the remaining mixture and recycled; it is the next lightest and forms no azeotropes. On the other hand, BD cannot be separated and recycled, at once, with

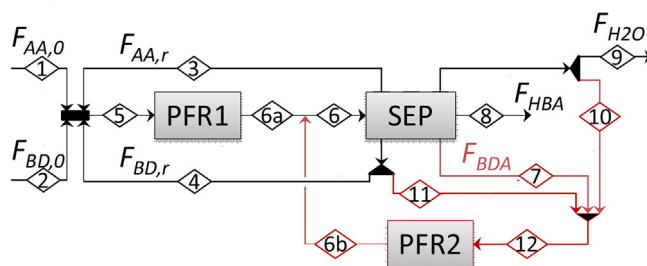
##### RSR-A



##### RSR-B



##### RSR-C

**Fig. 2 – Reaction–separation–recycle structures.**

AA (case in which, the plant may have one recycle stream). This is because of its azeotrope with HBA, which has a lower boiling temperature. Note that this is not possible even at pressures where BD is lighter than HBA. Since the composition of the two binary azeotropes (BD–HBA and BD–BDA) in the remaining mixture changes with pressure, BD can be separated by pressure-swing distillation and recycled to the reactor. Hence, RSR-A is a process in which the AA and BD reactants are recycled individually, while removing the water, HBA and BDA products from the process.

- The RSR-B structure retains the individual streams for recycling the reactants from the previous process (i.e., RSR-A),

but recycles also the BDA back to the reactor. The BDA recycle is mixed with the fresh BD before feeding it to the reactor. The idea is to keep the concentration of BDA high in the reactor to reduce its formation in the second equilibrium reaction; see Eq. (2). In other words, Le Chatelier's principle indicates that by adding BDA to the system, the reaction will favor the side opposing the addition of the species; namely, favoring the backward reaction.

- The RSR-C structure further retains the individual streams for recycling the reactants from the previous process (i.e., RSR-A), but converts BDA back to AA and HBA in a dedicated hydrolysis reactor. BDA is mixed with part of the water and part of the BD streams and reacted in a second reactor (PFR2). The outlet streams of both reactors are mixed and form the design basis of the separation system.

While all three processes share many similarities, there are key differences between these process concepts. Regarding the utilization of raw materials, the RSR-A process accepts the losses with the BDA; thus, this process is not 100% selective to the desired HBA product. The RSR-B process recycles BDA back to the esterification reactor, achieving 100% selectivity to HBA. The RSR-C process is also 100% selective, but BDA is converted back to its reactants in a dedicated hydrolysis reactor.

#### 4.2. Reactor size and preliminary operating point

Determining the reactor size means selecting the mass of catalyst that is able to convert the reactants for a given production capacity. The preliminary operating point defines the mass balance around the reactor and provides the starting point for designing the separation system.

These are achieved by means of a rough sensitivity analysis, showing the impact of the mass of catalyst, molar ratio of reactants at the reactor inlet and reaction temperature on AA conversion and HBA selectivity. This sensitivity reveals a rather large process operating window. The choice on the mass of catalyst, molar ratio and reaction temperature should show acceptable AA conversion and selectivity to HBA. The conversion is a trade-off between the mass of catalyst and recycle flow rate of reactants. In the RSR-A process, high HBA selectivity is required since any BDA formed is removed from the process; therefore, a loss of reactants. In the RSR-B process, the lower the HBA selectivity, the higher the recycle of BDA is expected; this leads to large recycles of BDA to the reactor, as well as operating the reactor at high BDA concentrations. In the RSR-C process, the lower the HBA selectivity, the larger the hydrolysis reactor (PFR2) is expected. These selections are detailed for the RSR-A process. For the RSR-B and RSR-C processes, a similar analysis is made (not presented here) based on which the reactor size and the preliminary operating point are determined. Here, only the results are presented.

The sensitivity analyses make use of a steady state model created in Aspen Plus. The reaction section is rigorously modeled using the reaction kinetics previously determined (Section 2.2), while the separation section uses an ideal separation model. The reactor is represented by the RPLUG block (i.e. a plug-flow reactor model), which assumes perfect radial mixing and neglects the axial mixing. Given a mass of catalyst, the operating policy (isothermal), the reaction kinetics and the inlet stream specifications (i.e. temperature, pressure, and alcohol to acid molar ratio), the RPLUG block solves rigorous mass and energy balance equations, together with phase-equilibrium relationships to calculate the condition of

the outlet stream. The separation is modeled by the SEP block, which simply distributes the components present in the inlet stream to several outlet streams (recycles and products); in this analysis, a complete separation is assumed (i.e., the products are removed from the process free of reactants, while the reactants are recycled free of products). The mass balance of fresh reactants and recycle is performed by the MIXER block.

The results for the RSR-A process are presented in Fig. 3. All data are generated for a fixed flow rate of fresh AA. Fig. 3 (top) shows the AA conversion ( $X_{AA}$ ) versus the amount of catalyst ( $m_{cat}$ ) at a reactor temperature of 100 °C and different BD/AA molar ratios at the reactor inlet. The conversion is sensitive with respect to catalyst amounts below roughly 1500 kg, and starts to drop significantly. In addition, Fig. 3 (middle-top) shows that the recycle of AA (and BD, not showed here) also starts to significantly increase below this amount of catalyst; note here the logarithmic y-axis. Coming back to the top figure, BD/AA molar ratios lower than 1 also lead to a significant loss of conversion. Additionally, Fig. 3 (middle-bottom) shows that, for the same reactor temperature, molar ratio below 2 significantly decreases the HBA selectivity ( $\sigma_{HBA}$ ). Fig. 3 (bottom) shows that operating the reactor at temperatures above 100 °C also leads to significant loss of selectivity, even when operating at high BD/AA molar ratios. One may add to this analysis the influence of recycling the reactants with small amounts of products; this is realistic since high-purity recycles might not be achievable due to increased separation costs.

As expected, trade-offs exist. This rough sensitivity analysis gives a fair understanding of the reactor behavior in various conditions and its operating window. Selecting a catalyst amount of 2500 kg provides a good balance between recycle of reactants and reactor size, as well as being sufficiently far from the high sensitivity region. Selecting a BD/AA molar ratio of 3 and an operating temperature of 100 °C keeps the HBA selectivity acceptable. This conservative operating point is indicated by the white dot in all graphs of Fig. 3.

For the RSR-B process, an amount of catalyst of 7500 kg is selected based on the results of a similar sensitivity analysis. This higher amount of catalyst (i.e., higher than that of the RSR-A process) is justified by the operation at high concentration of BDA, and therefore decreasing the reaction rate for HBA formation. The BD/AA molar ratio and reaction temperature are the same. For the RSR-C processes, the amount of catalyst for the esterification reactor (PFR1) is 2500 kg, while for the hydrolysis reactor (PFR2) is 5000 kg. The operating conditions of the esterification reactor are the same as for the RSR-A process. The hydrolysis reactor, for converting BDA back to its reaction products, operates at an inlet BDA/water molar ratio of 1, and BD/BDA close to 1/1.2. Temperature is the same, 100 °C. The mass balance of this preliminary operating point, for each process, is given in Table 3.

## 5. Process design

### 5.1. Design procedure

The design procedure is valid for each of these processes. The detailed process structure of the plant is developed considering the reaction and separation sections coupled by recycle (i.e. the RSR system). In addition, the recycle structures developed in Section 4.1 are maintained, the reactants being recycled separately. Thus, the characteristics of the RSR system previously described are preserved.



**Table 3 – Mass balance of the preliminary operating point for all three processes.**

RSR-A														
Stream	1	2	3	4	5	6	7	8	9					
Mole flows/kmol/h	17.7	16.8	1.1	39.5	75.0	75.0	0.9	15.8	17.7					
Mole fraction														
H <sub>2</sub> O								0.236						1
AA	1		1		0.25	0.014								
BD		1		1	0.75	0.526								
HBA						0.211			1					
BDA						0.012	1							
Mass flows/kg/h	1275	1511	76	3557	6419	6419	184	2282	319					
Mass fraction														
H <sub>2</sub> O								0.050						1
AA	1		1		0.210	0.012								
BD		1		1	0.790	0.554								
HBA						0.356			1					
BDA						0.029	1							
RSR-B														
Stream	1	2	3	4	5	6	7	8	9					
Mole flows/kmol/h	17.7	17.7	1.3	39.2	87.1	87.1	11.2	17.7	17.7					
Mole fraction														
H <sub>2</sub> O								0.203						1
AA	1		1		0.218	0.015								
BD		1		1	0.653	0.450								
HBA						0.203			1					
BDA						0.129	0.129	1						
Mass flows/kg/h	1275	1595	92	3535	8720	8720	2224	2551	319					
Mass fraction														
H <sub>2</sub> O								0.037						1
AA	1		1		0.157	0.011								
BD		1		1	0.588	0.405								
HBA						0.293			1					
BDA						0.255	0.255	1						
RSR-C														
Stream	1	2	3	4	5	6	6a	6b	7	8	9	10	11	12
Mole flows/kmol/h	17.7	17.7	1.4	39.6	76.4	83.2	76.4	6.8	2.4	17.7	17.7	2.4	2.0	6.8
Mole fraction														
H <sub>2</sub> O						0.241	0.236	0.300			1	1		0.35
AA	1		1		0.25	0.017	0.014	0.050						
BD		1		1	0.75	0.501	0.526	0.210					1	0.30
HBA						0.213	0.211	0.229		1				
BDA						0.028	0.012	0.211	1					0.35
Mass flows/kg/h	1275	1594	102	3571	6542	7236	6542	694	468	2551	319	43	183	694
Mass fraction														
H <sub>2</sub> O						0.050	0.050	0.053			1	1		0.061
AA	1		1		0.210	0.014	0.012	0.035						
BD		1		1	0.790	0.519	0.554	0.184					1	0.263
HBA						0.353	0.356	0.322		1				
BDA						0.065	0.029	0.406	1					0.675

While this design approach can easily fix the amount of catalyst and establish the size of the fixed-bed reactor for a given plant capacity and conversion, the design of the separation section requires a feed composition (reactor outlet) based on which the separation sequence can be developed and later on sized. A good starting point providing an initial mass balance is given by the preliminary operating point selected in Section 4.2. Rigorous thermodynamic analyses are used to develop the separation sequence.

The design pressure of the columns is set based on evaluating the VLE diagrams at different pressures and selected such that the temperature in the condenser allows using tower cooling water and the temperature in the reboiler allows using steam (one exception is C-3 in RSR-B which uses hot oil due to the higher temperature). Regarding the columns sizing, an initial value for the number of trays

and the feed stage are selected. Then, the product purity and recovery are selected. Based on these, the reflux ratio required to achieve the specified separation is calculated. The feed stage is selected such that the reboiler duty is minimized. Then, the number of stages is increased, and the procedure is repeated until no significant change in reboiler duty is noticed. This iterative procedure is used to design all columns.

From a separation standpoint, a key element present in all three processes is the difficult separation of the BD/HBA/BDA mixture. This was also observed by Yang et al. (2008b) in their experiments. The authors of that paper mention that “After the reaction, it is very difficult to obtain a high purity of HBA by general separation techniques such as distillation and extraction”. Note that their experiments focused on obtaining high purity HBA, not high selectivity, and conducted most of the reaction

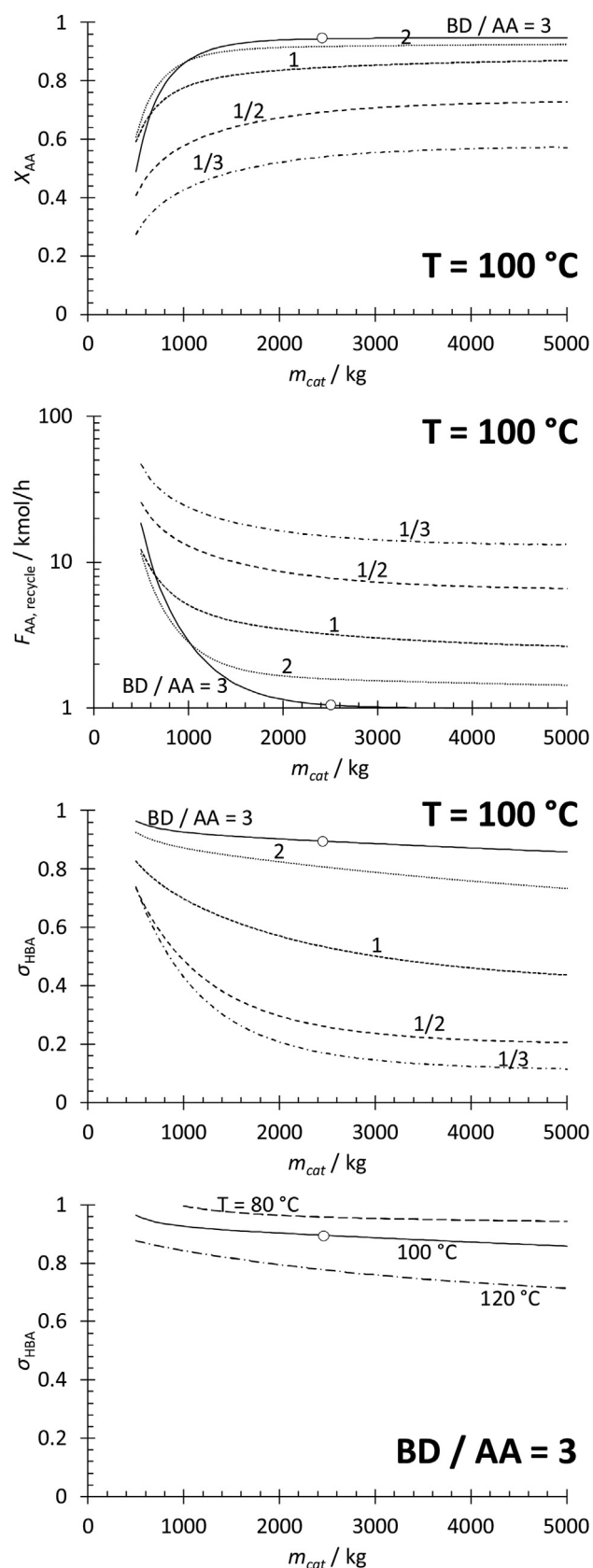


Fig. 3 – Process sensitivity with respect to key design and operating parameters.

experiments using excess of AA to achieve full conversion of BD.

## 5.2. RSR-A process

The complete process flow diagram and the mass balance are presented in Fig. 4. Fresh reactant AA is mixed with the AA recycle (stream 3a), while fresh reactant BD is mixed with the BD recycle (stream 3b). These streams are mixed and fed to the multi-tubular reactor PFR (36 tubes, 4 m length, 0.17 m diameter, 2500 kg catalyst). The reactor outlet consists of HBA, BDA, water and the remaining reactants, and it is fed to column C-1 where water (the lightest component in the mixture) is removed as top distillate product at over 99%wt purity. This is possible since water does not form any azeotropes at 0.2 bar, and therefore is easily removed from the process. The bottom stream of C-1 is mixed with a recycled stream (6) consisting mainly of BD and HBA, but also small amounts of AA. The mixed stream is fed to column C-2. Column C-2 recovers AA as distillate (stream 3A). This is possible since AA is the lightest component in the remaining mixture and forms no azeotropes. The bottom stream (8) of C-2 consists of BD, HBA and BDA. This mixture is difficult to separate due to presence of the binary azeotropes BD/BDA and BD/HBA. To make this difficult separation, a pressure-swing distillation system is used consisting of columns C-3 and C-4. The C-2 bottoms stream (8) and C-4 recycle stream (9) are mixed and form the feed stream (10) to the low-pressure column C-4 operated at 0.05 bar.

Fig. 5 presents the singular points and the distillation boundary of the BD/HBA/BDA system. At 0.05 bar, the concentration of the feed (stream 10) entering the distillation column C-3 falls in region I (Fig. 5, left diagram). Thus, BD is obtained as bottoms stream (3b) and recycled to the reaction section, while the distillate (stream 11, containing all three components) has a composition near the distillation boundary connecting the two binary azeotropes. At 0.8 bar, the locations of the binary azeotropes and distillation boundary change and the composition of the C-3 distillate (stream 11), which is the C-4 feed, falls in region II (Fig. 5, right diagram). Having crossed the distillation boundary, it is possible to obtain a bottoms stream (13) containing HBA and BDA, and a distillate stream (12) close to the distillation boundary. The former can be easily separated. The latter falls back in region I at lower pressure and can be recycled as feed to C-3. Note that about 15% of the C-4 distillate stream (12) is sent to C-2 to prevent accumulation of AA in the recycle loop C-2/C-3/C-4/C-2. This is because any AA that escapes C-2 via bottoms has no way out from the process, and it will start to accumulate in the aforementioned loop. The bottom stream of C-4 is fed to column C-5 that separates HBA as top distillate of over 99.5%wt purity (stream 14) and BDA as bottom product (stream 15). Overall, there are only two reactant streams AA (0a) and BD (0b) and three product streams: water (4), HBA (14) and BDA (15).

## 5.3. RSR-B process

The process flow diagram and mass balance of this process alternative are presented in Fig. 6. Fresh reactant AA is mixed with the recycle stream 3A (consisting of AA and water), while fresh reactant BD is mixed with the recycle streams 3B (mainly BD and some HBA) and 3C (mostly BDA). All these streams are mixed and fed to a multi-tubular reactor PFR (107 tubes, 4 m length, 0.17 m diameter, 7500 kg catalyst). The reactor outlet –

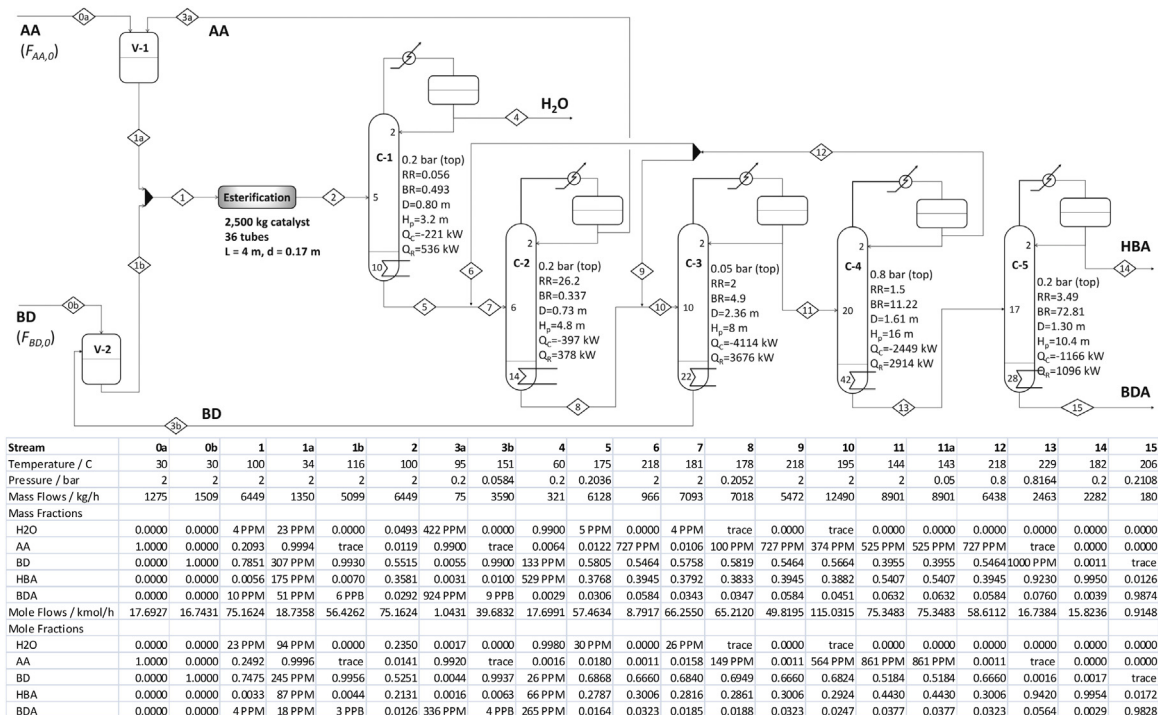


Fig. 4 – Process flow diagram and mass balance of the RSR-A process.

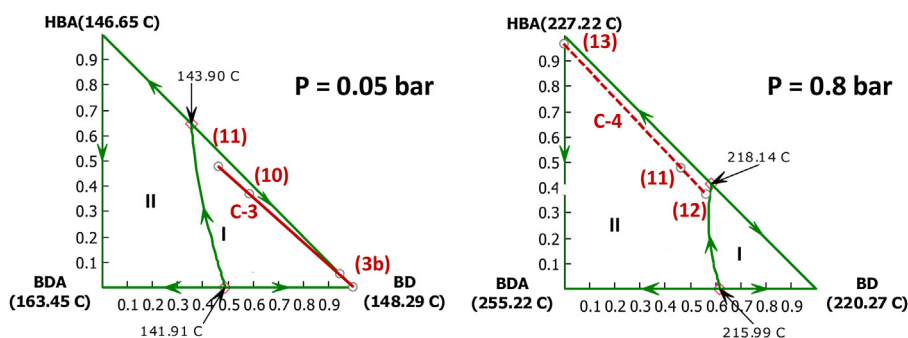


Fig. 5 – Separation by pressure-swing distillation of the BD/HBA/BDA mixture in the RSR-A and RSR-C processes: ternary maps with distillation boundaries showing the mass balance of the low-pressure column C-3 (left) and high-pressure column C-4 (right).

consisting of HBA, BDA, water, and the remaining reactants – is fed to column C-1 where water (the lightest component in the mixture) is removed as top distillate product at over 95%wt purity. The bottom stream (5) of C-1 is mixed with a recycled stream (6) consisting of BD and BDA, but also small amounts of AA, and then it is fed to column C-2. The recovered distillate of C-2 is a mixture of AA and water which is recycled (stream 3A), while the bottom stream of C-2 is mixed with a recycled stream (9), consisting of BD and BDA, and then fed to column C-3. As in the previous process, this BD/HBA/BDA mixture is very difficult to separate. Again, pressure-swing distillation is used.

However, the operation of column C-3 and C-4 is different since the feed to C-3 has a different composition when compared to that in the RSR-A process. The composition of this stream is very close to the distillation boundary at 0.05 bar, however at 0.8 bar falls well within region II (Fig. 7, left diagram). Therefore, in the RSR-B process, C-3 is the high-pressure column, while C-4 the low-pressure column. From C-3, it is possible to obtain an HBA/BDA mixture as bottoms (stream 12), free of BD, that can be split in column C-5 by simple distillation: the bottoms stream (3c) recovers the BDA and

recycles it to the reaction section, while HBA is recovered in the distillate (stream 14) at high purity. The distillate stream (11) of C-4 contains a mixture of HBA and BDA that has a composition near the distillation boundary connecting the two binary azeotropes. At 0.05 bar, the locations of the binary azeotropes and distillation boundary change and the composition of the C-3 distillate (stream 11), which is the C-4 feed, falls in region II (Fig. 7, right diagram). Having crossed the distillation boundary, it is possible to obtain a bottoms stream (3b) containing the reactant BD, which is recycled to reaction, and a distillate stream (13) close to the distillation boundary. This falls back in region II at high pressure and can be recycled as feed to C-3. Overall, there are only two reactant streams AA (0a) and BD (0b) and two product streams: water (4) and HBA (14). Note that in this case the BDA by-product is recycled to be converted to HBA.

#### 5.4. RSR-C process

Fig. 8 shows the process flow diagram and mass balance. Fresh reactant AA is mixed with recycled AA (stream 3A), while fresh reactant BD is mixed with recycled BD (streams 3B). These

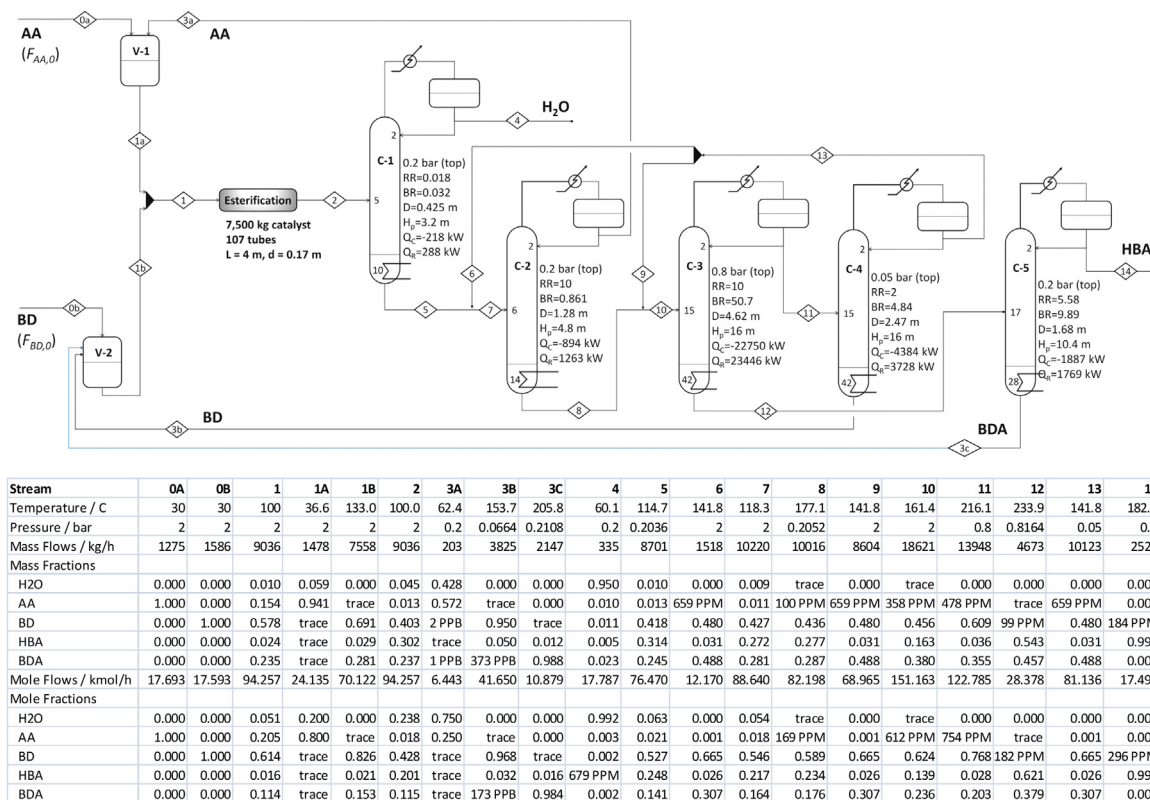


Fig. 6 – Process flow diagram and mass balance of the RSR-B process.

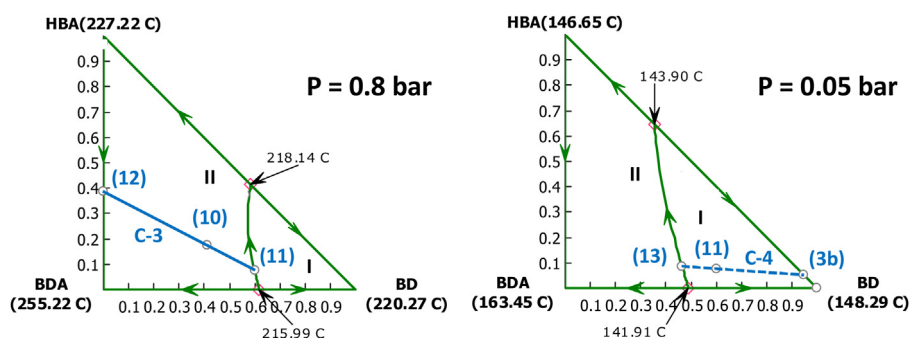


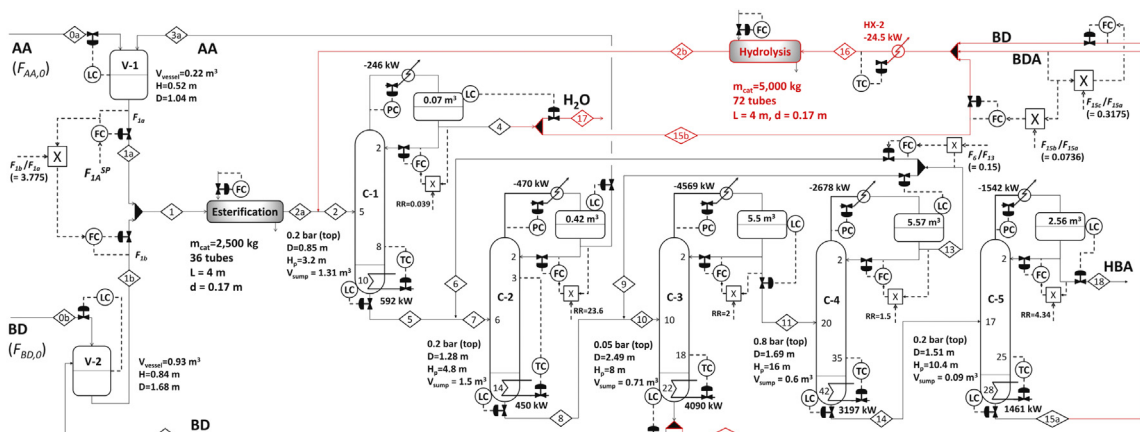
Fig. 7 – Separation by pressure-swing distillation of the BD/HBA/BDA mixture in the RSR-B process: ternary maps with distillation boundaries showing the mass balance of the high-pressure column C-3 (left) and low-pressure column C-4 (right).

streams are mixed and fed to a multi-tubular reactor PFR1 (36 tubes, 4 m length, 0.17 m diameter, 2500 kg catalyst). The reactor outlet – consisting of HBA, BDA, water, and the remaining reactants – is mixed first with the outlet of reactor PFR2 and then fed to column C-1 where water is removed as top distillate product at over 98%wt purity. The bottom stream of C-1 is mixed with a recycled stream (6) consisting of BD, HBA and some BDA, and then it is fed to column C-2. The recovered distillate of C-2 is AA which is recycled (stream 3A), while the bottom stream of C-2 is mixed with a recycled stream (9) consisting of BD, HBA and some BDA, and then fed to column C-3. The separation of the BD/HBA/BDA mixture is again made by pressure-swing in columns C-3 and C-4. Since the composition of the stream (3) feeding C-3 is very close to that in the RSR-A process, the separation steps are identical; one can follow the detailed description of the pressure-swing concept in Section 5.2.

The bottom stream of C-3 is BD (stream 15) which is split and mostly recycled (stream 3B) while the remaining part (stream 15C) is sent to the second reactor. The top part of C-3 is then separated in column C-4. The top product of C-4 (stream 13) is a mixture of BD, HBA and some BDA, which is recycled and split into stream 6 (added before C-2) and stream 9 (added before C-3). The bottom product of C-4 is sent to column C-5 which separates HBA (over 99.5%wt purity) as top distillate (stream 18). The bottom stream of C-5 (stream 15A) is mixed with stream 15B and 15C and cooled down to 100 °C, then fed to the hydrolysis multi-tubular reactor PFR2 (72 tubes, 4 m length, 0.17 m diameter, 5000 kg catalyst). The outlet of PFR2 is then mixed with the outlet of PFR1 and then fed to column C-1 (as described earlier). Overall, there are only two reactant streams AA (0A) and BD (0B) and two product streams: water (4) and HBA (18). Note that in this case the BDA by-

**Table 4 – Results of the economic evaluation of all three process alternatives.**

Cost	RSR-A	RSR-B	RSR-C
Capacity/[kt/y]	20.0	22.1	22.3
<b>Equipment (installed)/[\$]</b>			
PFR1	343,002	1,029,005	343,002
PFR2	–	–	686,003
C-1	443,800	397,100	446,600
C-2	447,900	547,400	471,800
C-3	869,100	6,105,100	917,100
C-4	903,200	1,181,200	986,100
C-5	624,000	765,400	670,600
Others	245,100	286,600	290,900
<b>Total</b>	<b>3,876,102</b>	<b>10,311,805</b>	<b>4,812,105</b>
<b>Utility/[\$/yr]</b>			
Electricity	46,661	78,112	47,818
Cooling	51,039	184,797	58,266
Heating	619,655	2,869,168	705,326
<b>Total/\$/y</b>	<b>717,354</b>	<b>3,132,077</b>	<b>811,409</b>
<b>Annualized and specific cost per unit product</b>			
TAC/[\$/y]	2,009,388	6,569,346	2,415,444
TAC specific/[\$/t]	100	297	109



Stream	0A	2	1	1A	1B	2A	3A	3B	4	5	6	7	8	9	10	11	12	13	14	16	17	18		
Temperature / C	30	100	100	35	115	100	95	151	60	175	217	180	178	217	195	143	151	217	229	100	60	182		
Pressure / bar	2	2	2	2	2	2	0.2	0.2	0.2	0.2036	2	2	0.2052	2	2	0.0584	0.8	0.8041	2	2	2	0.2		
Mass Flows / kg/h	1275	7233	6558	1374	5185	6558	99	3597	366	6867	1059	7927	7828	6004	13832	10056	3776	7063	2992	675	324	2539		
Mass Fractions																								
H2O	0.0000	0.0496	5 PPM	26 PPM	trace	0.0493	364 PPM	trace	0.5800	5 PPM	trace	4 PPM	trace	trace	trace	trace	trace	trace	trace	trace	trace	0.0608	0.9800	0.0000
AA	1.0000	0.0140	0.2093	0.9993	trace	0.0119	0.9900	trace	0.0108	0.0142	738 PPM	0.0124	100 PPM	738 PPM	377 PPM	518 PPM	738 PPM	trace	738 PPM	trace	671 PPM	0.0108	0.0000	0.0000
BD	0.0000	0.5174	0.7852	415 PPM	0.9931	0.5515	0.0058	0.9900	895 PPM	0.5449	0.5548	0.5462	0.5530	0.5548	0.5538	0.3900	0.9900	0.5548	1000 PPM	0.2629	895 PPM	0.0012	0.0000	0.0000
HBA	0.0000	0.3548	0.0055	170 PPM	0.0069	0.3582	0.0024	0.0100	861 PPM	0.3737	0.3449	0.3699	0.3745	0.3449	0.3616	0.4937	0.0100	0.3449	0.8450	0.0065	861 PPM	0.9950	0.0000	0.0000
BDA	0.0000	0.0641	22 PPM	105 PPM	15 PPB	0.0290	0.0015	21 PPB	0.0074	0.0671	0.0996	0.0715	0.0724	0.0996	0.0842	0.1158	21 PPB	0.0996	0.1540	0.6692	0.0074	0.0038	0.0000	
Mole Flows / kmol/h	17.6927	83.0024	76.4388	19.0577	57.3811	76.4388	1.3650	39.7616	19.9965	63.0059	9.5998	72.6057	71.2407	54.3987	125.6394	83.8977	41.7417	63.9984	19.8961	6.5605	17.7100	17.6021	0.0000	
Mole Fractions																								
H2O	0.0000	0.2400	26 PPM	104 PPM	trace	0.2350	0.0015	trace	0.9963	31 PPM	trace	27 PPM	trace	trace	trace	trace	trace	trace	trace	trace	trace	0.3472	0.9963	0.0000
AA	1.0000	0.0170	0.2492	0.9994	trace	0.0142	0.9922	trace	0.0028	0.0215	0.0011	0.0188	152 PPM	0.0011	576 PPM	863 PPM	trace	0.0011	trace	958 PPM	0.0028	0.0000	0.0000	
BD	0.0000	0.5003	0.7475	332 PPM	0.9957	0.5251	0.0046	0.9937	182 PPM	0.6590	0.6794	0.6617	0.6743	0.6794	0.6765	0.5187	0.9937	0.6794	0.0017	0.3000	182 PPM	0.0019	0.0000	
HBA	0.0000	0.2145	0.0033	85 PPM	0.0043	0.2132	0.0012	0.0063	109 PPM	0.2825	0.2640	0.2801	0.2854	0.2640	0.2762	0.4104	0.0063	0.2640	0.8815	0.0046	109 PPM	0.9953	0.0000	
BDA	0.0000	0.0282	9 PPM	38 PPM	6 PPB	0.0125	536 PPM	9 PPB	685 PPM	0.0369	0.0554	0.0394	0.0401	0.0554	0.0467	0.0700	9 PPB	0.0554	0.1169	0.3472	685 PPM	0.0028	0.0000	

**Fig. 8 – Process flow diagram, mass balance and plantwide control of the RSR-C process.**

product (15C) is converted in hydrolysis reactor PFR2 back into HBA product.

### 6. Process comparison

A rough economic evaluation and comparison between the three process alternatives is made. The aim is to indicate which process has the highest economic potential. This information may be further used in selecting a process for the purpose of future in-depth studies like heat integration and process dynamics.

The economic evaluation is made using the Aspen Process Economic Analyzer (APEA) in Aspen Plus V10. This involves sizing and cost estimating the equipment, as well as cal-

culating the utility consumption; the default APEA models, (sizing and cost equations, and utility prices) are used. The condensers of all columns use cooling water (30 °C inlet, 40 °C outlet), while reboilers use high-pressure steam (250 °C); one exception is C-3 reboiler in RSR-B which uses hot oil (280 °C inlet, 250 °C outlet).

The results are presented in Table 4. The RSR-A process seems to be the most efficient, having the lowest installed equipment and utility costs. These lead to a Total Annualized Cost (TAC) of 2 million \$ and a TAC specific cost of 100 \$/t of product. These are closely followed by the costs of the RSR-C process with a TAC of 2.4 million \$ and a TAC specific of 109 \$/t of product. By far, the RSR-B process shows the highest cost for installed equipment and is the most energy intensive. The main contribution to the installed costs is due to

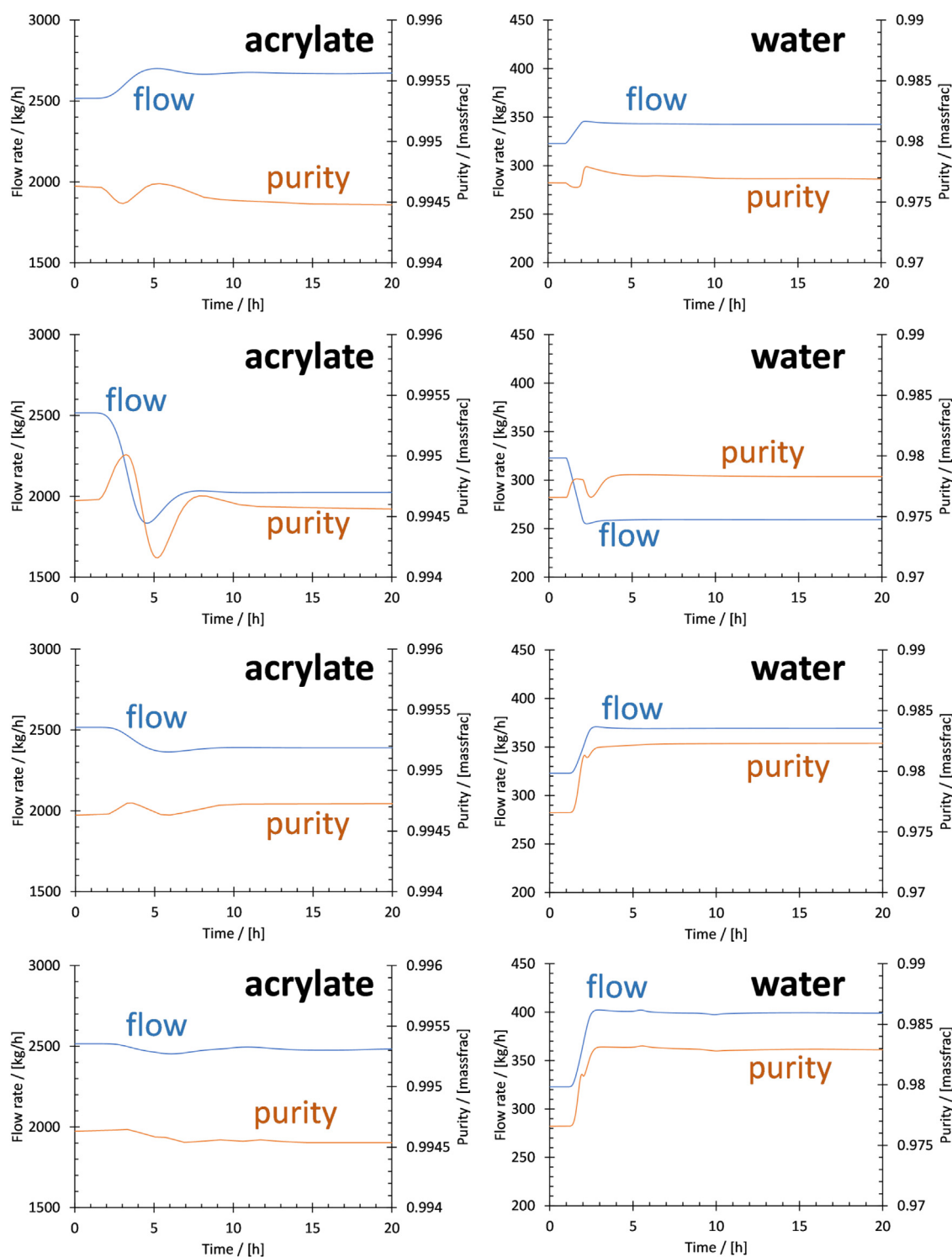


**Fig. 9** – Dynamic response to various process changes. Left/right diagrams: acrylate/water flow rates and purities. Top row diagrams: 7% increase of  $F_{1A}$  flowrate; middle-top row diagrams: 10% decrease of  $F_{1A}$  flowrate; middle-bottom row diagrams: contamination of fresh AA with 5% water; bottom row diagrams: contamination of fresh BD with 5% water.

the large reactor, C-3 and C-4 columns. As expected, due to high utility consumption, these two columns also have the largest contribution to the utility costs. These costs translate into a TAC of 6.6 million \$ and a TAC specific cost of 297 \$/t of product.

These results suggest that the RSR-A process should be further investigated. They also suggest that recovery of BDA may not be economically attractive, and may not justify the investment for the additional equipment. However, RSR-C pro-

cess may be considered a viable alternative from a material utilization standpoint.

## 7. Process control

The previous section shows that the RSR-A has the lowest total annual cost (investment and utilities), while the RSR-B is much more expensive. RSR-C is a viable alternative where raw-material utilization justifies the additional investment for BDA

conversion to HBA. On this basis, we select to evaluate in this section the controllability of the RSR-C process. Please note that from a controllability perspective, the RSR-A process is expected to pose less control related complexities compared to the RSR-C process. This is because RSR-C brings an additional recycle inside the separation section (due to BDA conversion to HBA), and therefore influencing the overall process dynamics. The controllability is assessed by rigorous dynamic simulation.

The plantwide control structure, presented in Fig. 8, follows from the considerations explained in detail in Dimian et al. (2014). Firstly, the control structure must ensure that each reactant is fed in the process in the right amount, avoiding accumulation or depletion. Since the HBA plant is a two-reactant process with the reactants being separately recycled, the recommended strategy is to fix the flow rate of one reactant at reactor-inlet (stream 1a in Fig. 8, containing high purity AA) and to use this flow rate as throughput manipulator. The reactor-inlet flow rate of the second reactant (stream 1b in Fig. 8, containing high purity BD) is ratioed to the first reactor-inlet flow. The fresh reactants are added such that the inventories in the buffer vessels V-1 and V-2 are kept constant. Increasing/decreasing the reactor-inlet flows leads to an increase/decrease of the amount of products. This strategy reduces the interactions between the reaction and the separation section, as it effectively cuts the two recycle loops.

Secondly, the control structure must ensure that the products HBA and water are separated at high purity and recovery and are removed from the plant. This is achieved by standard control of the distillation units, which is detailed later. Last but not least, the inventory of the by-product BDA must be controlled. Suppose that, due to a disturbance, the amount of BDA formed in the esterification reactor increases. Because the control of the separation section does not allow BDA to leave the plant, more BDA will be recovered and sent to the hydrolysis reactor. The general behavior of chemical reactors is that the reactant consumption rate increases when the reactant feed rate increases. Thus, the overall BDA inventory is self-regulating. However, the control system must ensure that the reaction conditions are roughly constant. For this reason, the ratios water/BDA and BD/BDA are kept constant at the inlet of the hydrolysis reactor.

The control of process units is quite standard. The reactors are operated at constant thermal agent flow rate (set at the maximum available value). As the heat effect of the reactions is small, the isothermal operation can be easily achieved for both reactors. For all distillation columns, the pressure is controlled by the condenser duty, reflux drum and sump levels are controlled by the distillate and bottoms rates, one temperature is controlled by the reboiler duty, while the reflux ratio is kept constant.

The holdup of the vessels is determined considering 10 min residence time. The dynamics of the heat exchangers is neglected. The PI-controllers are tuned by choosing reasonable ranges for the process variable (PV) and the controller output (OP) and then setting the controller gain to  $1 [\%OP \text{ range}] / [\%PV \text{ range}]$ . The integral time is set equal to an estimated time constant of the process. The column temperature controllers are tuned by assuming 1 min measurement delay, and using the ATV method to find the ultimate gain and the period of oscillations at stability limit and using the Tyreus–Luyben rules.

Fig. 9 shows the response of the process for various disturbances, which are introduced (one at a time) after 1 h of

steady state operation. The top two rows present results for changing the reactor-inlet acrylic acid flow rate, as flow rate and composition of plant outlet streams (acrylate, left diagram; water, right diagram). The bottom two rows show the same flow rates and compositions when fresh AA and fresh BD are contaminated with water. In all cases, it takes about 8 h until the disturbance is rejected. As expected, increasing/decreasing the reactor-inlet flow rate leads to higher/lower product rate. The flow rate of HBA product is lower when AA is contaminated with water (because AA is the throughput manipulator). Contamination of BD has little effect on HBA rate, because the control structure compensates the less pure fresh BD by an increase of its flow rate. More water in one of the plant-inlet streams is reflected by more water in the plant outlet. For all disturbances, the deviation from the steady state value of the HBA product purity is very small.

## 8. Conclusions

Production of 4-hydroxybutyl acrylate at industrial scale using conventional reaction–separation–recycle processes based on solid catalysts appears to be feasible. Fixed-bed tubular reactors and distillation-based equipment can achieve the required capacity and product purity. However, special systems like pressure-swing distillation needs to be employed to split the difficult alcohol/acrylate/diacrylate mixture. A general observation is that vacuum operation throughout the separation system is required to decrease the distillation temperature to suppress polymerization of the acrylate and acid. Another reason to operate at vacuum conditions is the selection of utilities.

The rough costs estimate for the installed equipment and utility consumption suggests that the RSR-A process has the highest potential. From a cost perspective, this result indicates that hydrolysis of the diacrylate by-product back to acrylate and acid is not necessarily needed. However, from a material utilization standpoint, the RSR-C process may be considered a viable alternative since it requires only one additional major equipment (i.e. the hydrolysis reactor) to perform the diacrylate hydrolysis; making the diacrylate recovery in the esterification reactor (as in the RSR-B process) is economically unfavorable.

Despite its complexity, the process is controllable. The control structure presented in this study is able to control the inventory of AA and BD reactants, BDA by-product, HBA and water products, and is efficient in rejecting various disturbances.

## Declaration of Competing Interest

The authors report no declarations of interest.

## Acknowledgment

AAK gratefully acknowledges the Royal Society Wolfson Research Merit Award (No. WM170003).

## Appendix A. Supplementary data

Supplementary material related to this article can be found, in the online version, at doi:<https://doi.org/10.1016/j.cherd.2021.11.040>.

## References

- BASF, 2016a. [Petrochemicals Specialty Monomers, Technical Information, TI/CP 1331e](#).
- BASF, 2016b. [Specialty Monomers, Technical Data, E-CPI/M 1610 Booklet](#).
- Curtis, M.A., 2008. A Process for the Production of Hydroxyalkyl (meth)acrylates, Patent No. EP1958930A2.
- Dimian, A.C., Bildea, C.S., Kiss, A.A., 2014. [Integrated Design and Simulation of Chemical Processes, second ed. Elsevier, Amsterdam](#).
- Dockner, T., Lermer, H., Bittins, K., Nestler, G., Brauch, G., 1995. Preparation of 1,4-butanediol Mono(meth)acrylate by Esterification of (meth)acrylic Acid with 1,4-butanediol, in Which an Aqueous Solution of Unconverted 1,4-butanediol is Obtained, Patent No. US5637760A.
- Jinno, H., Ishida, T., Takaki, H., Nakamura, M., 2015. Hydroxyalkyl (meth)acrylate and Method for Producing Same, Patent No. US20150126767A1.
- Moraru, M.D., Zaharia, E., Bildea, C.S., 2020. [Conceptual design of novel processes for 4-hydroxybutyl acrylate production. Comput. Aided Chem. Eng. 48, 1267–1272](#).
- Ostrowski, S., Jamróz, M.E., Dobrowolskia, J.Cz., 2011. [Formation of heavy adducts in esterification of acrylic acid: a DFT study. Comput. Theor. Chem. 974, 100–108](#).
- Sugiura, T., Okamura, K., Ito, K., Kawakami, N., Matsumoto, S., Matsuno, M., 2013. Process for Preparing 4-hydroxybutyl Acrylate, Patent No. WO 2013/157597.
- Tanaka, Y., Okamura, K., Ito, K., 2017. Process for Preparing 4-hydroxybutyl Acrylate, Patent No. US009670129B2.
- Tokuda, M., Kouno, M., Morioka, J., 2009. Method for Producing Hydroxyalkyl (meth)acrylate, Patent No. US8461374B2.
- Yang, J.I., Cho, S.H., Kim, H.J., Joo, H., Jung, H., Lee, K.Y., 2008a. [Production of 4-hydroxybutyl acrylate and its reaction kinetics over Amberlyst 15 catalyst. Can. J. Chem. Eng. 85, 83–91](#).
- Yang, J.I., Cho, S.H., Park, J., Lee, K.Y., 2008b. [Esterification of acrylic acid with 1,4-butanediol in a batch distillation column reactor over Amberlyst 15 catalyst. Can. J. Chem. Eng. 85, 883–888](#).